LRRK2 promotes the activation of NLRC4 inflammasome during *Salmonella* Typhimurium infection

Weiwei Liu,[1*] Xia'nan Liu,[1*] Yu Li,[1] Junjie Zhao,[3] Zhenshan Liu,[1] Zhuqin Hu,[1] Ying Wang,[1] Yufeng Yao,[2] Aaron W. Miller,[3,4] Bing Su,[1] Mark R. Cookson,[5] Xiaoxia Li,[3,6] and Zizhen Kang[1,3,6]

[1]Shanghai Institute of Immunology and [2]Department of Immunology and Microbiology, Shanghai Jiao Tong University School of Medicine, Shanghai, China
[3]Department of Immunology and [4]Department of Urology, Cleveland Clinic, Cleveland, OH
[5]Cell Biology and Gene Expression Section, Laboratory of Neurogenetics, National Institute on Aging, Bethesda, MD
[6]Department of Molecular Medicine, Cleveland Clinic Lerner College of Medicine, Case Western Reserve University, Cleveland, OH

Although genetic polymorphisms in the *LRRK2* gene are associated with a variety of diseases, the physiological function of LRRK2 remains poorly understood. In this study, we report a crucial role for LRRK2 in the activation of the NLRC4 inflammasome during host defense against *Salmonella enteric* serovar Typhimurium infection. *LRRK2* deficiency reduced caspase-1 activation and IL-1β secretion in response to NLRC4 inflammasome activators in macrophages. *Lrrk2*$^{-/-}$ mice exhibited impaired clearance of pathogens after acute *S.* Typhimurium infection. Mechanistically, LRRK2 formed a complex with NLRC4 in the macrophages, and the formation of the LRRK2–NLRC4 complex led to the phosphorylation of NLRC4 at Ser533. Importantly, the kinase activity of LRRK2 is required for optimal NLRC4 inflammasome activation. Collectively, our study reveals an important role for LRRK2 in the host defense by promoting NLRC4 inflammasome activation.

INTRODUCTION

The *leucine-rich repeat kinase 2* (*LRRK2*) gene is emerging as a genetic hotspot for disease associations. Pathogenic mutations in *LRRK2* are the most prevalent genetic alterations among Parkinson's disease (PD) patients (Paisán-Ruíz et al., 2004; Zimprich et al., 2004; Cookson, 2010), and single nucleotide polymorphisms in the *LRRK2* gene have been linked to a variety of inflammatory diseases including Crohn's disease, ulcerative colitis, and cancer (Barrett et al., 2008; Franke et al., 2010; Saunders-Pullman et al., 2010; Anderson et al., 2011; Inzelberg et al., 2012). These epidemiological evidences have instigated intense research efforts focusing on the pathogenic mechanisms of *LRRK2* variants with the ultimate goal of targeting LRRK2 for treatment.

Despite the growing literature on the roles of the *LRRK2* in disease development, much of its physiological function remains elusive (Chia et al., 2014; Cookson, 2015). The expression pattern of LRRK2 points to a critical function in the immune system. LRRK2 can be induced by IFN-γ stimulation in human monocytes, and it is preferentially expressed in mature macrophages and dendritic cells (Gardet et al., 2010). Consistently, accumulating evidence suggests that LRRK2 plays an important role in the host defense against the intracellular pathogens. In humans, an *LRRK2* missense single nucleotide polymorphism, which results in an unstable LRRK2 protein, has been shown to confer increased susceptibility to leprosy, a disease caused by *Mycobacterium leprae* infection (Zhang et al., 2009). In the mouse model, LRRK2 was required for the mucosal immunity against the *Listeria monocytogenes* (Zhang et al., 2015b). At the cellular level, LRRK2 was found to colocalize with intracellular *Salmonella enteric* serovar Typhimurium (*S.* Typhimurium) during bacterial infection in macrophages (Gardet et al., 2010). These evidences collectively indicate that LRRK2 is directly involved in the innate immune response against intracellular bacteria. However, the molecular mechanism by which LRRK2 contributes to the host immunity is unknown.

A major host response against the infection by intracellular bacteria is the activation of NLRC4 inflammasome (Amer et al., 2006; Sutterwala et al., 2007; Suzuki et al., 2007; Case et al., 2009; Miao et al., 2010a). For example, *S.* Typhimurium infection of macrophages induces NLRC4 inflammasome–mediated production of the proinflammatory cytokines IL-1β and IL-18 (Franchi et al., 2006; Miao et al., 2010b). Activation of NLRC4 inflammasome is initiated by the host recognition of cytosolic bacterial components such as flagellin or PrgJ, triggering the oligomerization of NLRC4 proteins (Miao et al., 2010b; Zhao et al., 2011). The NLRC4 oligomers nucleate the filament formation of the adapter protein ASC (apoptotic speck protein containing a caspase recruitment domain) and protease caspase-1 (Hu et

*W. Liu and X. Liu contributed equally to this paper.

Correspondence to Xiaoxia Li: lix@ccf.org; Zizhen Kang: kangz@ccf.org

Abbreviations used: ASC, apoptotic speck protein containing a caspase recruitment domain; CARD, caspase activation and recruitment domain; DSS, disuccinimidyl suberate; iBMDM, immortalized BMDM; LRR, leucine-rich repeat; MOI, multiplicity of infection; PCF, peritoneal cavity–flushed fluid; PD, Parkinson's disease; ROC, Ras of complex.

The Rockefeller University Press
J. Exp. Med. 2017 Vol. 214 No. 10 3051–3066
https://doi.org/10.1084/jem.20170014

al., 2015; Zhang et al., 2015a). Oligomerization of caspase-1 leads to proximity-induced proteolytic activation and subsequently results in the maturation IL-1β and IL-18 (Vance, 2015). Secreted IL-1β and IL-18 then recruit both the innate and adaptive immune system for the clearance of pathogens (Schroder and Tschopp, 2010).

In this study, we report that LRRK2 is essential for the optimal activation of NLRC4 inflammasome during *S.* Typhimurium infection. We found that the *LRRK2*-deficient macrophages showed diminished caspase-1 activation and reduced mature IL-1β secretion in response to NLRC4 inflammasome activators. In addition, *Lrrk2*$^{-/-}$ mice exhibited impaired ability to clear the pathogens during acute *S.* Typhimurium infection. Mechanistically, LRRK2 formed a complex with NLRC4 in response to *S.* Typhimurium infection. Structure–function analysis showed that LRRK2 interacted with NLRC4 via the WD40 domain and that the kinase activity of LRRK2 was required for full-scale caspase-1 activation and IL-1β secretion. Moreover, LRRK2 promoted the phosphorylation of NLRC4 at Ser533, a critical modification required for the assembly of NLRC4 inflammasome. In summary, our study discovered a novel role for LRRK2 in host defense against *S.* Typhimurium via promoting the activation of the NLRC4 inflammasome.

RESULTS

LRRK2 deficiency impairs NLRC4-dependent inflammasome activation

To determine the role of LRRK2 in NLRC4 inflammasome activation, we first examined the caspase-1 activation and IL-1β production in response to defined NLRC4 inflammasome activators in *LRRK2*-deficient and WT macrophages (Fig. 1, a–c and f). Cytosolic delivery of purified flagellin or PrgJ, two NLRC4 inflammasome–specific ligands, induced robust pro–caspase-1 and pro–IL-1β cleavage in the WT but not the *LRRK2*-deficient macrophages (Fig. 1, a, b, and f). Flagellin or PrgJ are both components of the intracellular pathogen *S.* Typhimurium. Consistently, we found that *LRRK2*-deficient macrophages also showed reduced ability to activate pro–caspase-1 and pro–IL-1β as compared with the WT cells in response to *S.* Typhimurium infection (Fig. 1, c and f).

Importantly, *LRRK2*-deficient macrophages resembled the WT cells in the ability to produce TNF in response to the tested stimuli (Fig. 1 d), indicating that the defect is specific to inflammasome activation. Additionally, we examined whether LRRK2 is involved in the activation of NLRP3 inflammasome besides NLRC4. We failed to detect noticeable differences between WT and *LRRK2*-deificient macrophages in their ability to activate NLRP3 inflammasome (Fig.1, e and f). LPS-primed WT and *LRRK2*-deficient macrophages showed a similar ability to activate caspase-1 and produce IL-1β in response to ATP or nigericin stimulation (Fig.1, e and f). Collectively, these data suggest that LRRK2 is specifically required for the optimal activation of the NLRC4 inflammasome.

LRRK2 is required for host defense against *S.* Typhimurium infection

We then sought to determine whether *LRRK2* deficiency also reduces NLRC4 inflammasome activation in vivo. A recent study reported that NLRC4-dependent IL-1β production from the neutrophils was crucial for protecting mice from acute *Salmonella* infection delivered through intraperitoneal injection (Chen et al., 2014). After a similar experimental design, we injected *Lrrk2*$^{-/-}$ and WT mice with 10^7 CFUs of *S.* Typhimurium intraperitoneally to induce peritonitis. IL-1β levels in the peritoneal cavity–flushed fluids (PCFs) and in the sera were significantly reduced in the *Lrrk2*$^{-/-}$ mice compared with that in the littermate control (WT) mice 6 h after infection (Fig. 2 a). The reduction in IL-1β production was associated with reduced infiltration of neutrophils (Fig. 2 b). Furthermore, the neutrophils sorted from infected *Lrrk2*$^{-/-}$ mice produced a smaller amount of IL-1β compared with WT controls (Fig. 2 c), suggesting impaired inflammasome activation in *Lrrk2*$^{-/-}$ neutrophils. Moreover, the reduction in IL-1β production was also associated with increased bacteria colonization in the peritoneal cavity (Fig. 2 d). A prior study showed that IL-1β is essential for controlling the bacteria infection in the *S.* Typhimurium–induced peritonitis model (Chen et al., 2014). Consistently, the bacterial colonization in the *Lrrk2*$^{-/-}$ mice was effectively attenuated by supplementing the mice with recombinant IL-1β through intraperitoneal injection (Fig. 2 e). Furthermore, although more than half of the WT mice remained alive 6 d after bacteria inoculation, 90% of the *Lrrk*$^{-/-}$ mice died 4 d after infection (Fig. 2 f). Collectively, these data indicate that *LRRK2* is required for the effective clearance of *S.* Typhimurium, which might be attributed to its role in promoting NLRC4-mediated IL-1β production.

LRRK2 deficiency reduces ASC speck formation upon NLRC4 inflammasome activation

A critical question is how LRRK2 regulates NLRC4 inflammasome activation. The activation of NLRC4 leads to the assembly of a macromolecule complex containing ASC and caspase-1. We analyzed the assembly of the NLRC4 inflammasome in *LRRK2*-deficient and control (WT) macrophages by immunoprecipitation of the endogenous ASC protein (the adapter for inflammasome complex) after *S.* Typhimurium infection (Fig. 3 a). Western blot analysis showed a substantial reduction of both NLRC4 and capase-1 in the inflammasome complex, suggesting that LRRK2 is required for the assembly of NLRC4 inflammasome (Fig. 3 a). The assembly of NLRC4 inflammasome concurs with the formation of ASC specks, which is required for NLRC4-mediated caspase-1 activation (Broz et al., 2010). We visualized the endogenous ASC specks in macrophages infected with *S.* Typhimurium (Fig. 3 b) or treated with purified flagellin using immunofluorescence staining (Fig. 3 c). The frequency of ASC speck–containing cells was decreased by 50% in *LRRK2*-deficient macrophages compared with

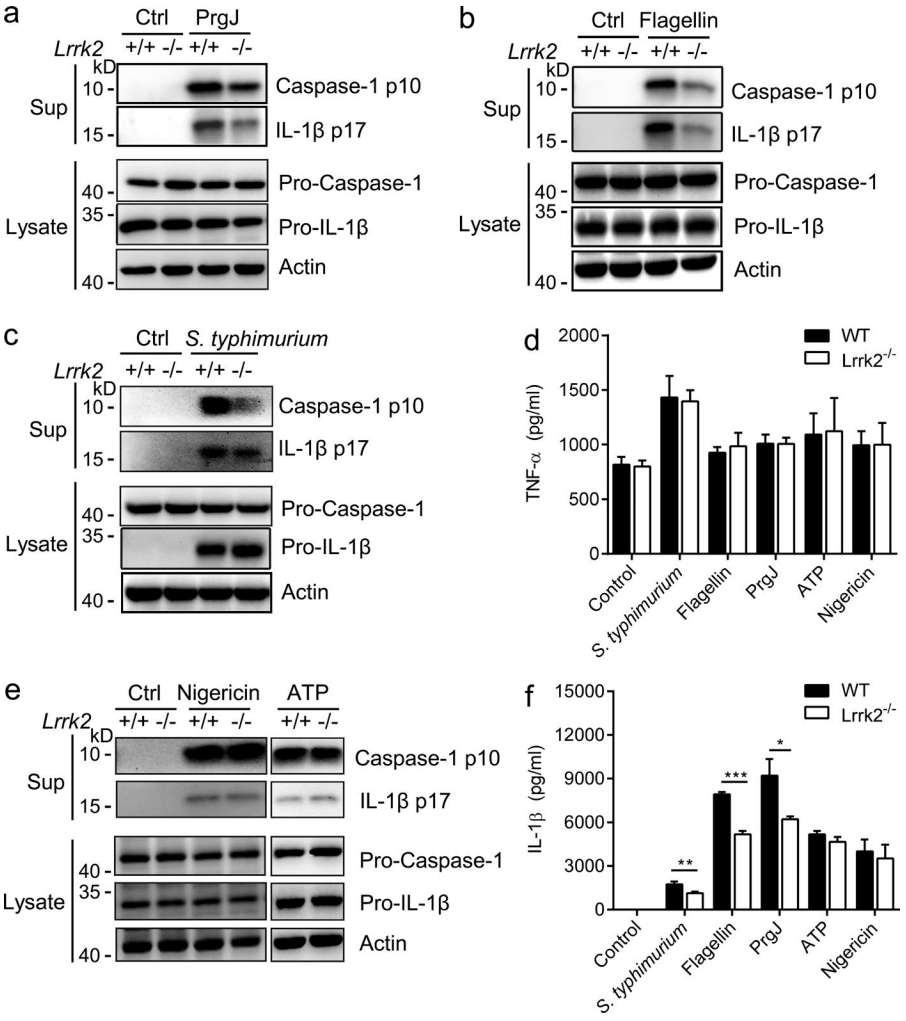

Figure 1. **LRRK2 is critical for NLRC4 inflammasome activation.** (a and b) LPS-primed WT and *Lrrk2*$^{-/-}$ peritoneal macrophages were treated with 1 µg/ml LFn-PrgJ and anthrax-protective antigen (PA; a) or 1 µg/ml LFn-flagellin + anthrax-protective antigen for 1 h (b). Cell lysates and culture supernatants (Sup) were collected and immunoblotted with the indicated antibodies. (c) Peritoneal macrophages from littermate control (WT) and *Lrrk2*$^{-/-}$ mice were infected with *S.* Typhimurium at an MOI of 100 for 2 h. Cell lysates and culture supernatants were collected and immunoblotted with the indicated antibodies. (d) ELISA of TNF-α in cell-free supernatants from WT and *Lrrk2*$^{-/-}$ peritoneal macrophages that were either infected with *S.* Typhimurium at an MOI of 100 for 2 h or pretreated with LPS (500 ng/ml) for 4 h followed by stimulation with LFn-flagellin + anthrax-protective antigen (1 µg/ml), LFn-PrgJ anthrax-protective antigen (1 µg/ml), ATP (5 mM), or nigericin (20 µM) for 1 h. (e) WT and *Lrrk2*$^{-/-}$ peritoneal macrophages were primed with 500 ng/ml LPS for 4 h and then treated with ATP (5 mM) or nigericin (20 µM) for 1 h. Cell lysates and culture supernatants were collected and immunoblotted with the indicated antibodies. "Ctrl" indicates the control group. (f) ELISA of IL-1β in cell-free supernatants from WT and *Lrrk2*$^{-/-}$ peritoneal macrophages that were treated as stated in d. Data are shown as means ± SEM; *, $P < 0.05$; **, $P < 0.01$; ***, $P < 0.001$; determined by Student's *t* test; all conditions were determined in triplicate. In each panel, data are representative of at least three independent experiments.

that in the WT controls (Fig. 3, b and c), suggesting that LRRK2 is required for ASC speck formation upon NLRC4 inflammasome activation.

Biochemical studies have determined that the ASC specks are oligomers of ASC protein that manifest as Triton X-100–insoluble aggregates (Masumoto et al., 1999; Hara et al., 2013). We prepared Triton X-100–soluble and Triton X-100–insoluble fractions from WT and *LRRK2*-deficient macrophages infected with *S.* Typhimurium (Fig. 3 d) or transfected with flagellin (Fig. 3 e). The Triton X-100–insoluble fractions were treated with the cross-linking agent disuccinimidyl suberate (DSS) to analyze the oligomerization of ASC. Consistent with decreased ASC speck formation in *LRRK2*-deficient macrophages (Fig. 3, b and c), the formation of the ASC dimer and oligomer in *LRRK2*-deficient macrophages was largely reduced compared with that in the WT controls (Fig. 3, d and e). Collectively, these data indicate that LRRK2 deficiency reduces the formation of ASC specks in response to NLRC4 inflammasome activation.

WD40 of LRRK2 and LRR of NLRC4 are required for LRRK2–NLRC4 interaction

The reduced ASC speck formation in *LRRK2*-deficient macrophages prompted us to further examine the interaction between the LRRK2 and NLRC4 inflammasome pathways. Upon *S.* Typhimurium infection, both NLRC4 and NLRP3 inflammasomes are activated (Man et al., 2014; Qu et al., 2016). However, coimmunoprecipitation experiments indicated that LRRK2 only formed a complex with NLRC4 but not NLRP3 in macrophages after *S.* Typhimurium infection (Fig. 4 a). Consistently, LRRK2 specifically pulled down NLRC4 but not NLRP3 or ASC in HEK293T cells (Fig. 4 b), suggesting that LRRK2 may specifically interact with NLRC4. Indeed, recombinant LRRK2 protein was able to form a complex with purified NLRC4 in vitro (Figs. 4 c and S1). LRRK2 is a large cytosolic protein consisting of a leucine-rich repeat (LRR) domain, a Ras of complex (ROC) GTPase domain, a C terminus of ROC (COR) domain, a kinase domain, and a WD40 repeat domain. We performed structure–function analysis to determine the relative contribu-

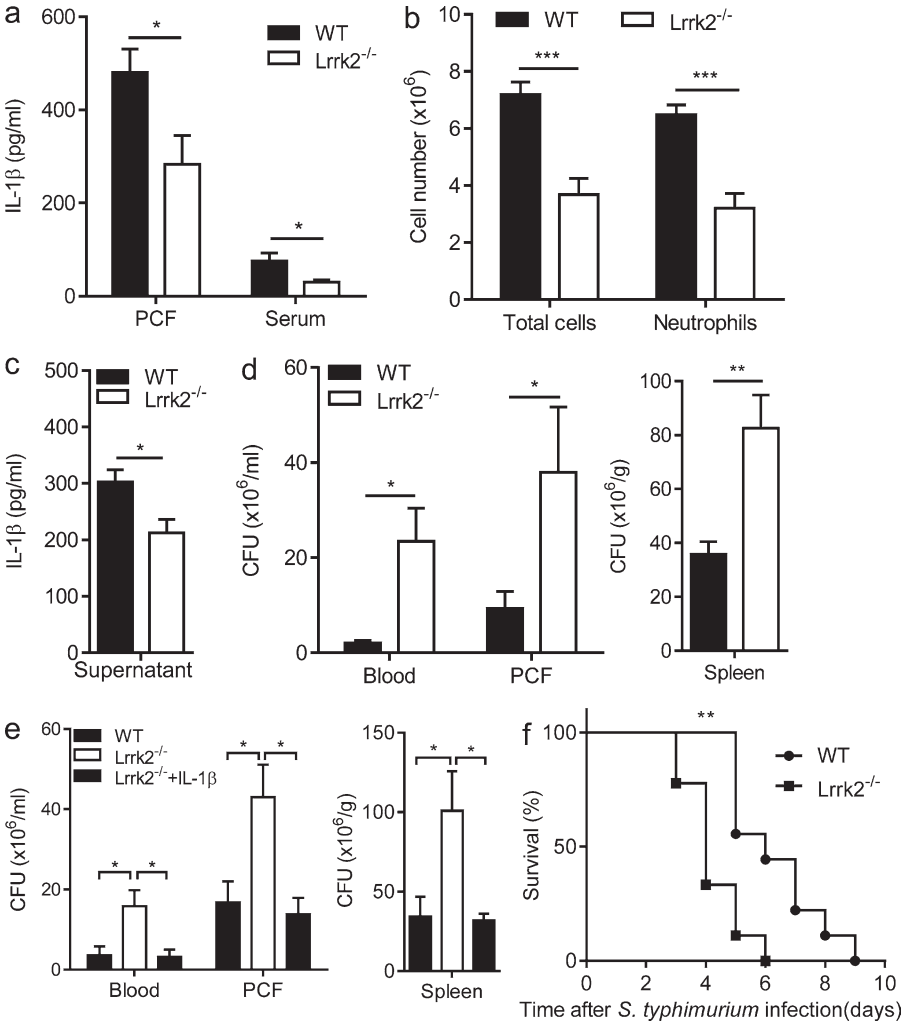

Figure 2. ***Lrrk2*$^{-/-}$ mice are more susceptible to *S.* Typhimurium–induced peritoneal inflammation.** (a) ELISA analysis of IL-1β levels in PCF and sera of littermate control (WT) and *Lrrk2*$^{-/-}$ mice 6 h after *S.* Typhimurium infection. (b) Absolute number of total peritoneal cells and neutrophils ($CD11b^+$ $Ly6G^+$) from PCF of WT and *Lrrk2*$^{-/-}$ mice 6 h after *S.* Typhimurium infection. (c) ELISA analysis of IL-1β from supernatants of an overnight-cultured equal number of neutrophil cells isolated from flushed peritoneal cells of WT and *Lrrk2*$^{-/-}$ mice, which were infected by *S.* Typhimurium for 6 h. (d) Bacterial burden in blood, PCF, and spleens of WT and *Lrrk2*$^{-/-}$ mice 24 h after *S.* Typhimurium infection. (e) Mice were administered with PBS or recombined mouse IL-1β (250 ng/mouse) for 4 h followed by *S.* Typhimurium infection for 24 h. Bacterial burden in blood, PCF, and spleens were monitored by serial dilution. (f) Survival of littermate control (WT) and *Lrrk2*$^{-/-}$ mice infected intraperitoneally with *S.* Typhimurium (10^2 CFUs/mouse). *, $P < 0.05$; **, $P < 0.01$; ***, $P < 0.001$; determined by Student's *t* test (a–e) or the Kaplan-Meier method (f). Data in a–e are representative of three independent experiments, and $n = 5$ mice/group; data in f are representative to two independent experiments, and $n = 12$ mice/group.

tions from the different domain or domains to the interaction with NLRC4. Using overexpressed full-length and different domains of LRRK2, we found that LRRK2 interacted with NLRC4 primarily via the WD40 domain (Fig. 4 d). In addition, we generated deletion mutants of NLRC4 lacking the caspase activation and recruitment domain (CARD; ΔCARD), the LRR domain (ΔLRR), or both the CARD and LRR domains (ΔCARD + LRR) and tested their ability to interact with LRRK2. Interestingly, deleting the LRR domain of NLRC4 was sufficient to abolish its interaction with LRRK2 (Fig. 4 e). Further analysis showed that the WD40 domain of LRRK2 formed a complex with the LRR domain of NLRC4 when coexpressed in 293T cells, implicating them as the interacting surfaces for the LRRK2 and NLRC4 (Fig. 4 f). The crystal structure of NLRC4 suggests that the NLRC4 LRR domain sequesters the protein as a monomeric state in an auto-inhibitory conformation (Hu et al., 2013). The LRR deletion leads to a constitutively active NLRC4 in processing of IL-1β. Therefore, our data imply that LRRK2 may be required for releasing the self-inhibition of NLRC4 to activate inflammasome assembly.

Kinase activity of LRRK2 is required for NLRC4 inflammasome activation

Interestingly, the LRRK2 kinase inhibitor GSK2578215A (Reith et al., 2012; Saez-Atienzar et al., 2014) greatly reduced the formation of the endogenous LRRK2–NLRC4 complex in *S.* Typhimurium–infected macrophages (Fig. 4 g). Pretreatment with the LRRK2 inhibitors (LRRK2–IN-1 [Deng et al., 2011] or GSK2578215A) noticeably attenuated ASC polymerization, caspase-1 activation, and IL-1β cleavage in *S.* Typhimurium–infected peritoneal macrophages (Fig. 5, a and b). Of note, LRRK2 inhibitors prevented the phosphorylation of LRRK2 at Ser935 in macrophages, an event previously shown to correlate with suppression of LRRK2 kinase activity (Fig. 5 b). Furthermore, these LRRK2 inhibitors were able to suppress the caspase-1 activation and pro–IL-1β cleavage induced by the NLRC4 inflammasome activator flagellin (Fig. 5 c), implicating the kinase activity of LRRK2 in NLRC4 inflammasome activation.

To validate this observation, we reconstituted NLRC4 inflammasome components in HEK293T cells, which allowed us to test LRRK2 mutants with defective and enhanced ki-

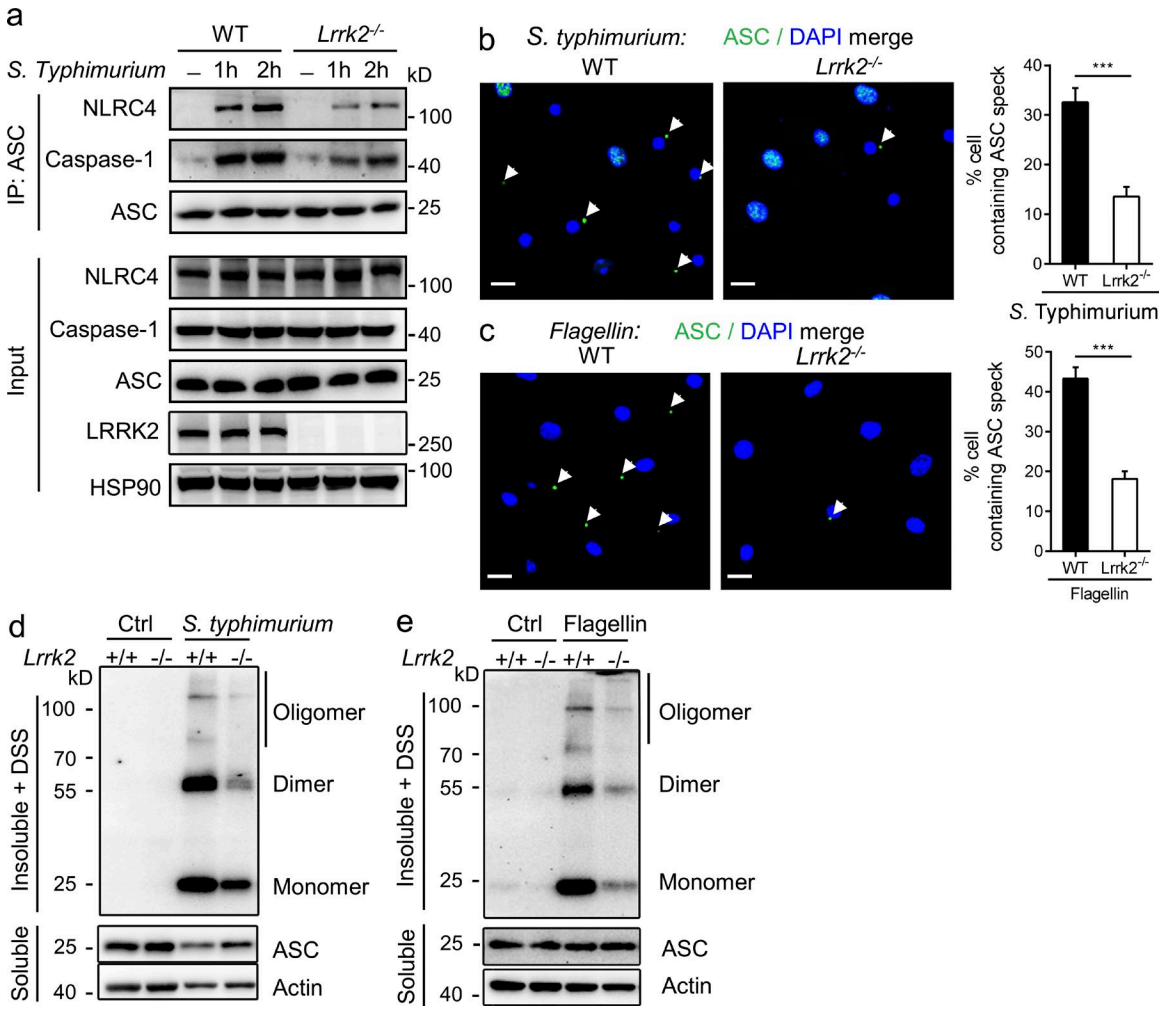

Figure 3. **LRRK2 promotes ASC speck formation and assembly of NLRC4 inflammasome.** (a) Peritoneal macrophages from littermate control (WT) and *Lrrk2*$^{-/-}$ mice were infected with *S.* Typhimurium at an MOI of 50 for 1 or 2 h. After cross-linking with DTBP, cell lysates were immunoprecipitated (IP) with anti-ASC antibody and immunoblotted with the indicated antibodies. Whole-cell lysates are shown as the input. (b and c) LPS-primed WT and *Lrrk2*$^{-/-}$ peritoneal macrophages were either infected with *S.* Typhimurium at an MOI of 50 (b) or cytosolic delivery of 1 µg/ml LFn-flagellin (c). ASC speck formation was assayed by ASC immunofluorescent staining, and cells were counterstained by DAPI (blue). Fluorescent images were analyzed by confocal microscopy. Percentages of macrophages containing ASC foci was quantified (right), with at least 200 cells counted in each experiment. Each condition was performed in triplicate. Quantitative data are shown as means ± SEM; ***, $P < 0.001$; determined by Student's test. Arrowheads mark ASC specks. Bars, 10 µm. (d) Peritoneal macrophages from littermate control (WT) and *Lrrk2*$^{-/-}$ mice were infected with *S.* Typhimurium at an MOI of 50 for 1 h. Cells were dissolved with Triton X-100–containing buffer followed by cross-linkage of insoluble fractions with DSS to capture ASC oligomers. Immunoblots of those insoluble fractions (Insoluble + DSS) and soluble fractions were detected with an antibody to ASC. (e) Immunoblot analysis of ASC in cross-linked Triton X-100–insoluble fractions from LPS-primed WT and *Lrrk2*$^{-/-}$ macrophages treated with 1 µg/ml LFn-flagellin + anthrax-protective antigen (PA) for 30 min. All results are representative of three independent experiments.

nase activity. In the reconstituted system, although overexpression of WT LRRK2 significantly increased caspase-1 activation (Fig. 5 d) and IL-1β secretion (Fig. 5 e), the kinase-dead mutant LRRK2 D2017A (Johnson et al., 1996; Nolen et al., 2004; Matikainen-Ankney et al., 2016) failed to promote IL-1β production (Fig. 5, d and e). In contrast, the PD-associated G2019S *LRRK2* mutant, which possesses enhanced kinase activity (Zimprich et al., 2004; Inzelberg et al., 2012), exhibited increased ability to induce IL-1β production compared with the WT protein (Fig. 5, d and e). These data suggest that LRRK2 promotes NLRC4 inflammasome activation through its kinase activity. We then sought to confirm this finding by testing macrophages expressing WT and *LRRK2* mutants. Because primary macrophages are resistant to viral transduction, we used CRISPR-Cas9 to generate *LRRK2*-deficient immortalized BMDMs (iBMDMs). The *LRRK2*-deficient iBMDMs were restored with WT LRRK2, LRRK2 G2019S (hyperactive), LRRK2 D2017A (kinase

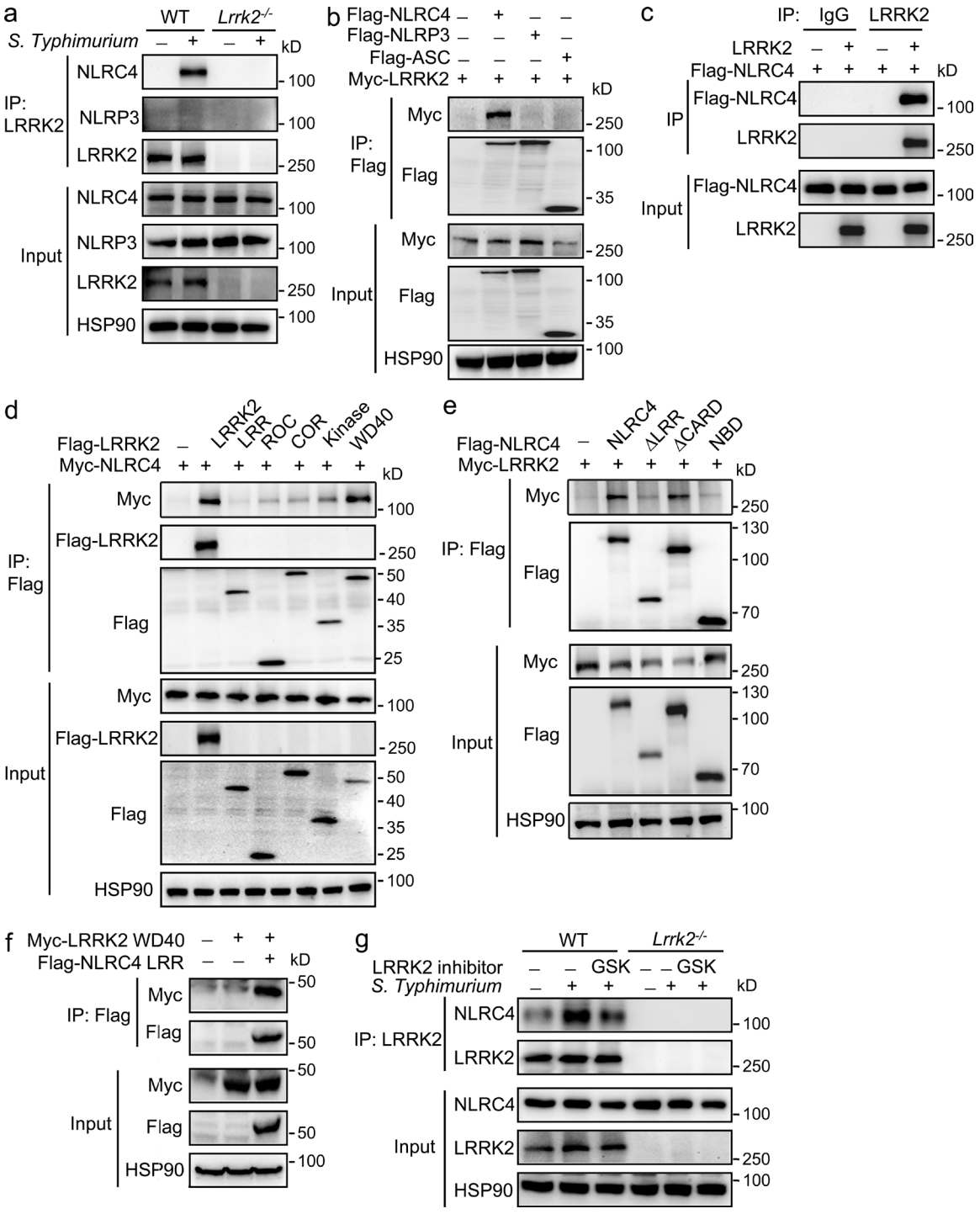

Figure 4. **LRRK2 directly interacts with NLRC4 to promote inflammasome assembly.** (a) Peritoneal macrophages from WT and *Lrrk2*$^{-/-}$ mice were infected with *S.* Typhimurium at an MOI of 50 for 45 min. Uninfected cells were included as controls. Cell lysates were then immunoprecipitated (IP) using anti-LRRK2 antibody and were immunoblotted with the indicated antibodies. Whole-cell lysates are shown as the input. (b) LRRK2 interacts with NLRC4 but not NLRP3 and ASC. The HEK293T cells were transfected with Myc-tagged LRRK2 and cotransfected with/without Flag-tagged NLRC4, NLRP3, or ASC as indicated. Cell lysates were immunoprecipitated with anti-Flag and analyzed by immunoblot. (c) In vitro pull-down assay using recombinant LRRK2 and NLRC4 proteins: 50 ng purified 3×Flag-NLRC4 protein was incubated with 200 ng recombinant LRRK2 protein followed by immunoprecipitation with anti-LRRK2 antibody and Western blot analysis. (d) Flag-tagged WT full-length LRRK2 or different LRRK2 domains (LRR, ROC, C terminus of ROC [COR], kinase, and WD40) were coexpressed with Myc-tagged NLRC4 in 293T cells, immunoprecipitated with anti-Flag, and analyzed by immunoblot. (e) Flag-tagged full-length NLRC4 and the NLRC4 mutants ΔLRR (NLRC4 lacking LRR domain), ΔCARD (NLRC4 lacking CARD), or only nucleotide-binding domain (NBD) do-

dead), or empty vectors. Consistent with our finding in the reconstituted system, the LRRK2 D2017A (kinase dead) failed to restore ASC oligomerization (Fig. 5 f), caspase-1 activation, and IL-1 β cleavage (Fig. 5 g) in response to *S.* Typhimurium infection, whereas the hyperactive LRRK2 G2019S mutant showed an enhanced ability to promote inflammasome activation (Fig. 5, f and g) in the iBMDMs. Collectively, our results demonstrate that the kinase activity of LRRK2 is required for NLRC4 inflammasome activation.

LRRK2 phosphorylates NLRC4 at Ser533 upon inflammasome activation

The reduced ASC speck formation in *LRRK2*-deficient macrophages (Fig. 3) indicated that ASC oligomerization was impaired in the absence of LRRK2 during NLRC4 inflammasome activation. Biochemical evidence suggests that formation of ASC oligomers is triggered by and subsequently to the activation of NLRC4 protein (Broz et al., 2010). A critical step in the activation of NLRC4 is the phosphorylation at the Ser533 on NLRC4 (Qu et al., 2012; Matusiak et al., 2015). Because LRRK2 forms a complex with NLRC4 and the kinase activity of LRRK2 is required for optimal NLRC4 inflammasome activation, we hypothesize that LRRK2 may promote NLRC4 phosphorylation.

To determine LRRK2-mediated NLRC4 modification, we performed tandem mass spectrometry analysis for NLRC4 protein immunoprecipitated from LRRK2 and NLRC4–coexpressing HEK239 cells. With 66% of the NLRC4-unique peptides captured from the sample, pSer533 was the only phosphorylated residue detected (Fig. S2, a and b). In support of this, NLRC4 Ser533 phosphorylation was significantly attenuated in the *LRRK2*-deficient macrophages in response to NLRC4 inflammasome activators (Fig. 6, a–c). Moreover, overexpression of LRRK2 enhanced phosphorylation of WT NLRC4 but not NLRC4 S533A in HEK293T cells (Fig. 6 d). Consistently, immunoprecipitated LRRK2 from HEK293T cells induced the phosphorylation of purified NLRC4 (Fig. 6 e). Correlated with exaggerated NLRC4 inflammasome activation (Fig. 5, d and e), LRRK2 G2019S protein showed an enhanced ability to promote NLRC4 Ser533 phosphorylation compared with the WT protein (Fig. 6 e). However, the LRRK2 kinase-dead mutant D2017A failed to induce NLRC4 phosphorylation (Fig. 6 e). These data suggest that NLRC4 may be a direct substrate for LRRK2. PKCδ was the first kinase identified to phosphorylate NLRC4 Ser533 during *S.* Typhimurium infection (Qu et al., 2012). Using PKCδ as a positive control, recombinant LRRK2 was indeed able to phosphorylate NLRC4 at Ser533 (Figs. 6 f and S1). Consistently, LRRK2 inhibitors suppressed LRRK2- but not PKCδ-induced NLRC4 Ser533 phosphorylation in the in vitro kinase assay (Fig. 6 g). We noted that LRRK2 deficiency did not completely abolish the phosphorylation of NLRC4, suggesting that an additional kinase or kinases may contribute to NLRC4 phosphorylation (Fig. 6, a–c). Knockdown of PKCδ in *LRRK2*-deficient BMDMs further attenuated NLRC4 Ser533 phosphorylation and completely abolished caspase-1 and pro–IL-1β cleavage (Fig. 6 h), suggesting that LRRK2 and PKCδ may play complementary roles in phosphorylating NLRC4 at Ser533 and promoting NLRC4 inflammasome activation.

LRRK2 kinase activity is required for host defense against *S.* Typhimurium infection

Given the critical role of LRRK2-mediated NLRC4 Se533 phosphorylation during NLRC4 inflammasome activation, we tested whether LRRK2 kinase activity is required for host defense against *S.* Typhimurium infection. To this end, we used the intraperitoneal injection of the *S.* Typhimurium model in which LRRK2 is required for NLRC4-dependent IL-1β production and pathogen clearance (Fig. 2). Intraperitoneal injection of the LRRK2 inhibitor GSK2578215A 1 h before infection completely abolished LRRK2 Ser935 phosphorylation in peritoneal cells from *S.* Typhimurium–infected mice (Fig. 7 a). IL-1β levels in the PCF and in the sera were significantly reduced in the LRRK2 inhibitor–treated mice compared with that in the control mice (Fig. 7 b). The reduction in IL-1β production was associated with reduced cell infiltration in the peritoneal cavity (Fig. 7 c) and increased colonization and dissemination of bacteria (Fig. 7 d).

Next, we took advantage of a transgenic mouse strain that carries a hyperactive *LRRK2* mutant gene, the *LRRK2* G2019S, to further validate the physiological function of LRRK2 kinase activity during host defense. Genotyping of *LRRK2* G2019S transgenic mice by RT-PCR and sequencing of cDNA from macrophages and brain tissues suggested human LRRK2 G2019S expression (Fig. S3). Restoration of *LRRK2*-deficient iBMDMs with LRRK2 G2019S led to enhanced NLRC4 inflammasome activation after *S.* Typhimurium infection (Fig. 5 g). Consistently, macrophages from transgenic mice expressing LRRK2 G2019S showed exaggerated caspase-1 activation, IL-1β production, and ASC polymerization in response to *S.* Typhimurium infection compared with the littermate controls (Fig. 7, e and f). The *LRRK2* G2019S transgenic mice also exhibited enhanced IL-1β production (Fig. 7 g), increased cell infiltration (Fig. 7 h), and improved pathogen clearance (Fig. 7 i) in response to acute

main were coexpressed with Myc-tagged LRRK2 in HEK293T cells, immunoprecipitated with anti-Flag, and analyzed by immunoblot. (f) Flag-tagged NLRC4 LRR domain was coexpressed with Myc-tagged LRRK2 WD40 domain in 293T cells followed by immunoprecipitation with anti-Flag antibody and immunoblot analysis. (g) LPS-primed peritoneal macrophages from littermate control (WT) and *Lrrk2*$^{-/-}$ mice were treated with LRRK2 inhibitor GSK2578215A (GSK) at 2 µM for 1 h and then infected with *S.* Typhimurium at an MOI of 50 for 1 h. Cell lysates were subjected to co-immunoprecipitation with anti-LRRK2 antibody followed by Western blotting. Whole-cell lysates are shown as the input. All the results are representative of at least three independent experiments.

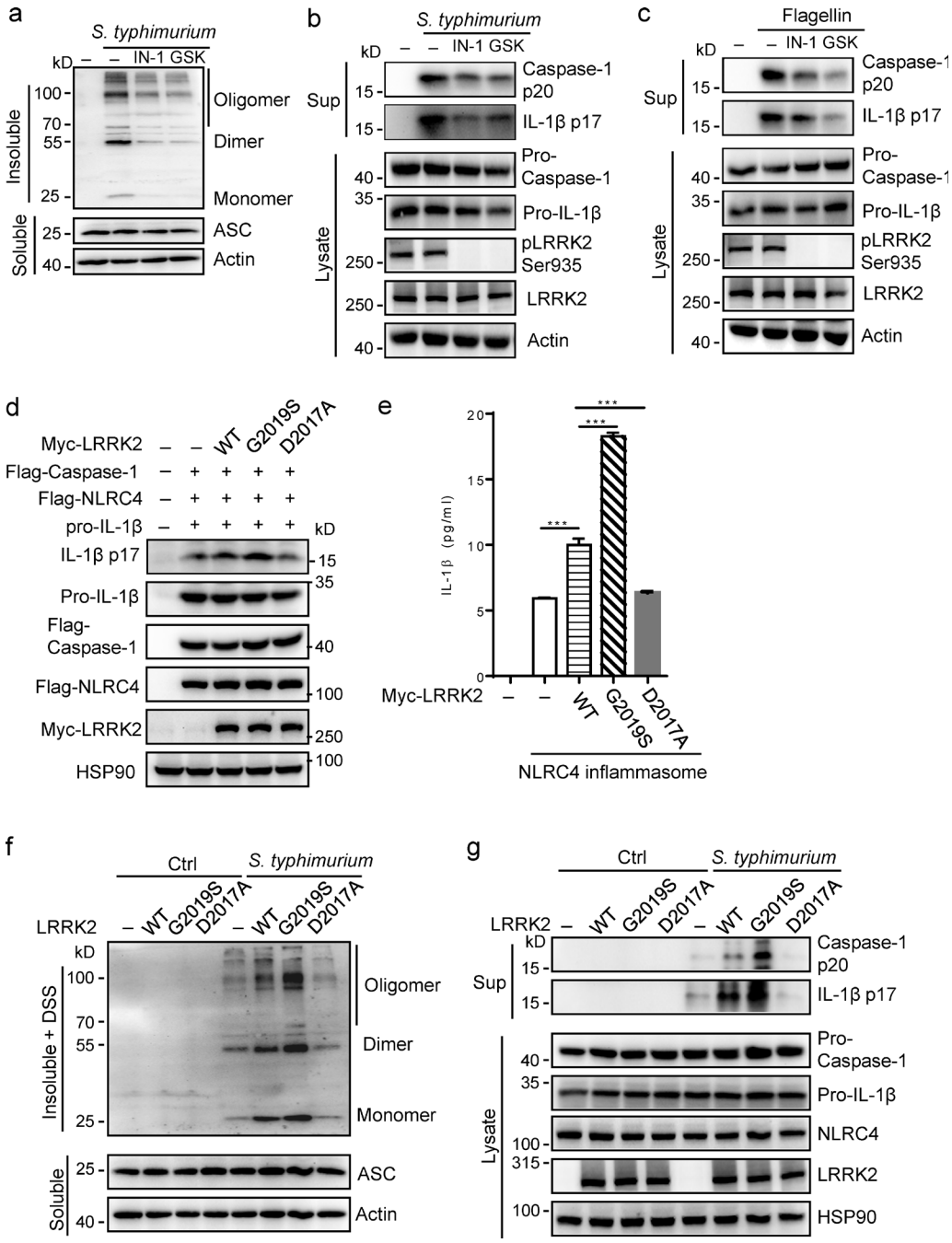

Figure 5. **LRRK2 kinase activity is required for NLRC4 inflammasome activation.** (a) LPS-primed peritoneal macrophages were treated with LRRK2 inhibitors 2 µM LRRK2–IN-1 (IN-1) or 2 µM GSK2578215A for 1 h and then infected with *S.* Typhimurium at an MOI of 50 for 1 h. Cells were lysed with Triton X-100–containing buffer followed by cross-linkage of insoluble fractions with DSS to capture ASC oligomers. Insoluble fractions (Insoluble + DSS) and soluble fractions were detected with antibody to ASC by immunoblot. (b and c) LPS-primed macrophages were treated with LRRK2 inhibitors either by 2 µM LRRK2–IN-1 or 2 µM GSK2578215A for 1 h and then infected with *S.* Typhimurium at an MOI of 100 for 2 h (b) or stimulated with 1 µg/ml LFn-flagellin and anthrax-protective antigen (PA) for 1 h (c). Cell lysates and culture supernatants (Sup) were collected and blotted with the indicated antibodies. (d and e) Reconstitution of the NLRC4 inflammasome activation in HEK293T cells: HEK293T cells were plated in six-well microplates. The cells were transfected with plasmids expressing Flag-tagged human pro–IL-1β (500 ng/well), pro–caspase-1 (300 ng/well), and NLRC4 (500 ng/well) with or without plasmid encoding Myc-tagged LRRK2 (1,500 ng/well) or its G2019S or D2017A mutants for 24 h. IL-1β cleavage was assessed by immunoblot (d) and ELISA analysis of IL-1β level (e) in the supernatants. Data are shown as means ± SEM; ***, $P < 0.001$; determined by one-way ANOVA followed by Bonferroni's post hoc test. (f) *LRRK2*-deficient iBMDMs were generated by CRISPR-Cas9–mediated deletion. For rescue experiments, Myc-tagged human LRRK2 WT, G2019S, or D2017A mutants were stably expressed in the *LRRK2*-deficient iBMDMs. These cells were primed with LPS and then infected with *S.* Typhimurium at an MOI of

S. Typhimurium infection in the peritoneal cavity. Collectively, these data show that LRRK2 kinase activity is required for host defense against *S.* Typhimurium infection.

DISCUSSION

In this study, we report an important physiological role for LRRK2 in the host defense against *S.* Typhimurium infection. We found that the activation of NLRC4 but not NLRP3 inflammasome was impaired in *LRRK2*-deficient macrophages. *Lrrk2*$^{-/-}$ mice exhibited decreased IL-1β production after *S.* Typhimurium infection, resulting in increased bacterial colonization and a higher mortality rate. Mechanistically, LRRK2 was shown to be in a complex with NLRC4 in macrophages after *S.* Typhimurium infection, implicating the LRRK2–NLRC4 interaction during NLRC4 inflammasome activation. In support of this, *LRRK2* deficiency blunted NLRC4 Ser533 phosphorylation induced by NLRC4 inflammasome activators, and the kinase activity of LRRK2 is required for the optimal activation of NLRC4 inflammasomes. Moreover, the in vitro kinase assay showed that purified LRRK2 was able to promote the phosphorylation of NLRC4 at Ser533. In summary, our study identified a novel function of LRRK2 as a critical kinase for NLRC4 activation during the host defense response.

The activation of NLRC4 is an important biochemical event during NLRC4 inflammasome activation. A previous study has shown that the LRR domain helps to sequester NLRC4 in an autoinhibitory conformation (Hu et al., 2013). We found that the LRR domain of NLRC4 is required for its interaction with LRRK2 (Fig. 4 e). It is possible that the LRR domain of NLRC4 mediates the interaction with LRRK2. The binding of LRRK2 to the LRR domain of NLRC4 might result in conformational change that activates NLRC4, permitting subsequent phosphorylation and oligomerization of NLRC4.

Our data also indicate that the kinase activity of LRRK2 is required for the optimal activation of the NLRC4 inflammasome (Fig. 5). The kinase activity of LRRK2 has been of particular interest because most of the pathogenic *LRRK2* mutations appear to have increased kinase activity (Rudenko et al., 2012). Intriguingly, we found that expression of *LRRK2* G2019S, the most common pathogenic mutant associated with PD, enhanced caspase-1 activation and IL-1β production in response to NLRC4 inflammasome activation (Fig. 7, e and f). This observation is consistent with the emerging concept of PD as an inflammatory disease. A recent study showed that increased serum levels of IL-1β effectively identified asymptomatic *LRRK2* G2019S carriers from noncarrier controls in humans (Dzamko et al., 2016). Furthermore, higher IL-1β concentration in the serum predicted increased risk for developing PD among the asymptomatic carriers. This observation is consistent with studies reporting the polymorphism of the *IL-1b* gene with PD susceptibility in humans (Wahner et al., 2007; Arman et al., 2010). Furthermore, previous studies have demonstrated a pathogenic role of IL-1β in mouse model of PD (Pott Godoy et al., 2008; Rodrigues et al., 2014). Collectively, our findings may also provide a novel pathogenic mechanism by which LRRK2 G2019S induces PD development in human.

MATERIALS AND METHODS

Mice

Lrrk2$^{-/-}$ mice (C57BL/6N-*Lrrk2*$^{tm1.1Mjff/J}$; approved by the Michael J. Fox Foundation for Parkinson's Research; JAX stock 016121) and *LRRK2* G2019S transgenic mice (Tg[*LRRK2**G2019S]^{1Cjli}; JAX stock 009609) were purchased from The Jackson Laboratory and backcrossed onto a C57BL/6 background for at least six generations. All mice were bred and maintained in individually ventilated cages under specific pathogen-free conditions in accredited animal facilities. 8–10-wk-old gender-matched littermate control mice were used as controls for all experiments. All animal procedures were performed in compliance with protocols approved by the Institutional Animal Care and Use Committee of Shanghai Jiao Tong University School of Medicine.

Reagents and antibodies

LPS (*Escherichia coli* serotype 0111:B4), flagellin from *S.* Typhimurium, and ATP (A2383) were purchased from Sigma-Aldrich. Poly(dA:dT) and nigericin were from InvivoGen. Anthrax-protective antigen, LFn-flagellin, and LFn-PrgJ were gifts from F. Shao (National Institute of Biological Sciences, Beijing, China). Anti–ASC (N-15)–R, anti–caspase-1 p10 (M20), normal rabbit IgG, and normal mouse IgG were from Santa Cruz Biotechnology, Inc. Anti–mouse caspase-1 (p20), ASC, and NLRP3 antibodies were from Adipogen. Anti-NLRC4 antibody was from EMD Millipore. Anti-NLRC4 and NLRC4 (p-Ser533) antibodies were from ECM Biosciences. Anti–mouse IL-1β antibody (AF-401-NA) was from R&D Systems. Anti–human IL-1β antibody and anti-LRRK2 antibody were from Abcam. Anti-Flag antibody was from Sigma-Aldrich. Anti-Myc antibody was from Cell Signaling Technology. Anti-actin and -HSP90 antibodies were from Proteintech. LRRK2 inhibitors LRRK2–IN-1 and GSK2578215A were purchased from Selleckchem. Antibodies for flow cytometry (FITC-Ly6G and PE-CD11b [M1/70]) were purchased from eBioscience. All antibodies were used at a dilution of 1:1,000,

50 for 1 h. Cells were dissolved with Triton X-100–containing buffer followed by cross-linkage of insoluble fractions with DSS to capture ASC oligomers. Insoluble fractions (Insoluble + DSS) and soluble fractions were detected with antibody to ASC by immunoblot. (g) *LRRK2*-deficient iBMDMs were restored with Myc-tagged human LRRK2 WT, G2019S, or D2017A mutants and then infected with *S.* Typhimurium at an MOI of 100 for 2 h. Cell lysates and culture supernatants were collected and blotted with the indicated antibodies. All the data are representative of three independent experiments.

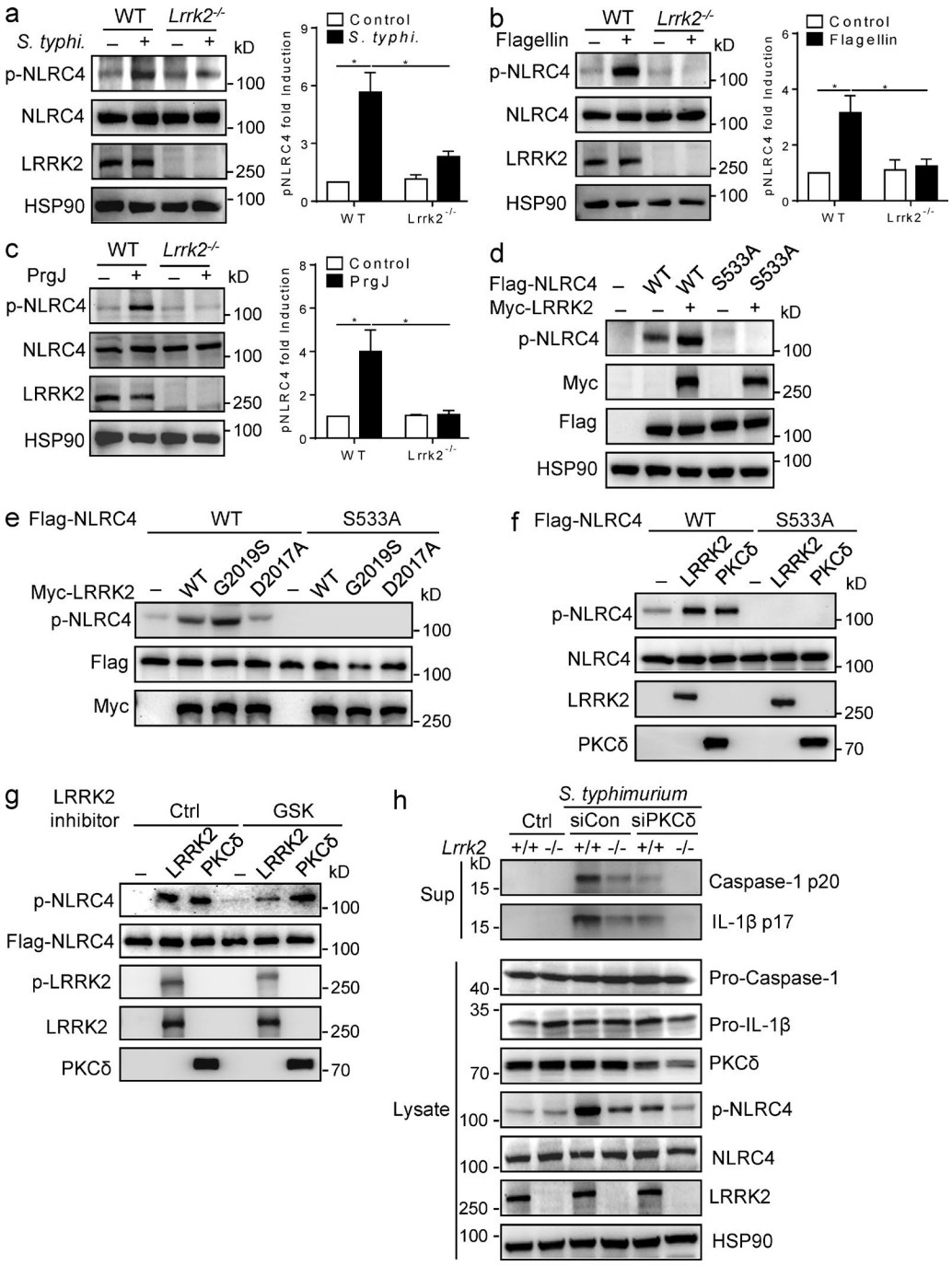

Figure 6. **LRRK2 phosphorylates NLRC4 Ser533 for NLRC4 inflammasome activation.** (a–c) BMDMs from littermate control (WT) and *Lrrk2*$^{-/-}$ mice were infected with *S.* Typhimurium at an MOI of 50 for 1 h (a) and then stimulated with 1 µg/ml LFn-flagellin and anthrax-protective antigen (PA) for 30 min (b) or 1 µg/ml LFn-PrgJ and PA (c) for 20 min. Cell lysates were collected and blotted with the indicated antibodies. Relative quantitation of NLRC4 phosphorylation was performed by ImageJ. Each relative pNLRC4 value was normalized to total NLRC4 protein and to the WT control. Each condition was performed at least in triplicate. Data are shown as means ± SEM; *, $P < 0.05$; determined by Student's *t* test. (d) Flag-tagged WT or NLRC4 mutant S533A were coexpressed with Myc-tagged LRRK2 in HEK293T cells. Cell lysates were collected and blotted with the indicated antibodies. (e) In vitro kinase assay. Immunoprecipitated Myc-tagged LRRK2 WT, G2019S, or D2017A were mixed with purified Flag-tagged WT or NLRC4 mutant S533A (50 ng as substrates), respectively. pNLRC4 and protein inputs were analyzed by immunoblot. (f) In vitro kinase assay. Purified human LRRK2 (200 ng) or PKCδ protein (50 ng) were mixed with immunoprecipitated Flag-tagged WT or NLRC4 mutant S533A (50 ng as substrates), respectively. NLRC4 phosphorylation was analyzed by immunoblot. (g) In vitro kinase assay with inhibitors. Purified recombinant LRRK2 (200 ng) or PKCδ protein (50 ng) were treated with LRRK2 inhibitor GSK2578215A (GSK) and mixed with purified Flag-tagged WT NLRC4 (substrates). NLRC4 phosphorylation and protein inputs were analyzed by immunoblot.

and all chemical reagents were bought from Sigma-Aldrich unless otherwise specified.

Cell culture

Unless otherwise indicated, all cells were cultured at 37°C in 95% air and 5% CO_2. Peritoneal macrophages were elicited by intraperitoneal injection of 1 ml BBL thioglycollate medium, brewer modified (4%; BD), and then they were recovered 4 d later by peritoneal lavage with 5 ml PBS. The peritoneal macrophages were cultured in DMEM cell culture medium (Gibco) containing 10% FBS (Gibco), 1% penicillin, and streptomycin. BMDMs were obtained from bone marrow of the tibia and femur and cultured in DMEM with 20% FBS, 20 ng/ml mouse M-CSF (PeproTech), and penicillin/streptomycin for differentiation and proliferation. Cells were differentiated for 6 d and then replated and used for experiments the next day. HEK293T cells were cultured in DMEM cell culture medium containing 10% FBS, 1% penicillin, and streptomycin.

Salmonella infection in vitro

The *S.* Typhimurium (14028; ATCC) strain was grown in Luria-Bertani medium at 37°C for overnight culture. Overnight-cultured bacteria were diluted at 1:100 and cultured for another 3 h to induce SPI-1 expression. Bacteria were added to macrophages at a multiplicity of infection (MOI) of 50–100, and gentamycin (50 μg/ml) was added after 30 min to kill the remaining extracellular bacteria.

Inflammasome activation

To induce inflammasome activation, 1×10^6 cells were plated in a 12-well plate overnight, and the medium was changed to Opti-MEM the next morning before stimulation. For NLRP3 inflammasome activation, the cells were primed with LPS (500 ng/ml) for 4 h. After that, the cells were stimulated with ATP (5 mM) or nigericin (10 μM) for 1 h. For NLRC4 inflammasome activation, cells were either infected with *S.* Typhimurium (MOI 50–100) or purified *S.* Typhimurium flagellin (2 μg/ml; Sigma-Aldrich) was delivered in the cytosol using DOTAP following the manufacturer's protocol (Roche). Alternatively, cells were treated with anthrax-protective antigen (1 μg/ml) and 1 μg/ml LFn-flagellin or LFn-PrgJ. For all experiments, cells were lysed with 1% NP-40 supplemented with complete protease inhibitor cocktail (Roche), and cell-free supernatant was either collected for ELISA analysis or concentrated with methanol and chloroform for immunoblot.

Plasmids

The plasmid pCMV-2×Myc-*LRRK2* expressing either Myc-tagged WT or mutant G2019S was purchased from Addgene (plasmids 25361 and 25362). cDNAs encoding human pro–IL-1β, ASC, and pro–caspase-1 were inserted into the mammalian expression vector pCMV-3×Flag. *LRRK2* WT and various domains mutants or *NLRC4* WT and domain deletion mutants were also cloned into pCMV-3×Flag vector. *NLRC4* mutant S533A construct was generated by site-directed point mutagenesis. All constructs were confirmed by sequencing.

Generation of *LRRK2* knockout iBMDMs by CRISPR-Cas9–mediated genome editing

The immortalized macrophage line iBMDMs derived from C57BL/6 mice (Shi et al., 2015) were provided by F. Shao. Lentiviral CRISPR-Cas9 targeting guide RNA–expressing vector (lentiCRISPRv2) was obtained from Addgene (52961). The *LRRK2*-knockout target sequence used was 5′-TTAGTGAGAACCCACACGTG-3′. To generate *LRRK2*-knockout iBMDMs, lentiviruses containing the *LRRK2* target sequence were used to transduce iBMDMs. Puromycin-positive iBMDMs were used by a limited dilution assay for single clones. Candidate knockout clones were screened by the T7 endonuclease I-cutting assay and identified by immunoblotting with anti-LRRK2 antibody.

Reconstitution of *LRRK2*-deficient iBMDMs

LRRK2-deficient iBMDMs were transfected with Myc-tagged *LRRK2* WT or mutants using Lipofectamine 2000 (Thermo Fisher Scientific). After 3 d, transfected cells were selected with Geneticin (Gibco) for 1–2 wk. Expression of reconstituted LRRK2 proteins was determined by immunoblot.

siRNA-mediated interference

Primary WT and *Lrrk2*$^{-/-}$ BMDM in 12-well cell culture plates were transfected with 25 μM siRNA using Lipofectamine RNAiMAX (Thermo Fisher Scientific). The siRNA specific for mouse PKCδ (SMARTpool) and the scrambled siRNA were bought from GE Healthcare. The knockdown efficiency was determined by immunoblot.

Cytokine measurements

Supernatants from cell cultures, serum, or PCF were analyzed for mouse IL-1β, IL-18, IL-6, or TNF with ELISA kits from eBioscience. All procedures followed the manufacturer's instructions.

(h) Primary BMDMs from littermate control (WT) and *Lrrk2*$^{-/-}$ mice were transfected with scramble control siRNA (siCon) or siRNA-targeting PKCδ (siPKCδ) and stimulated with LPS plus *S.* Typhimurium infection. Cell lysates and culture supernatants (Sup) were collected and blotted with the indicated antibodies. All data are representative of three independent experiments.

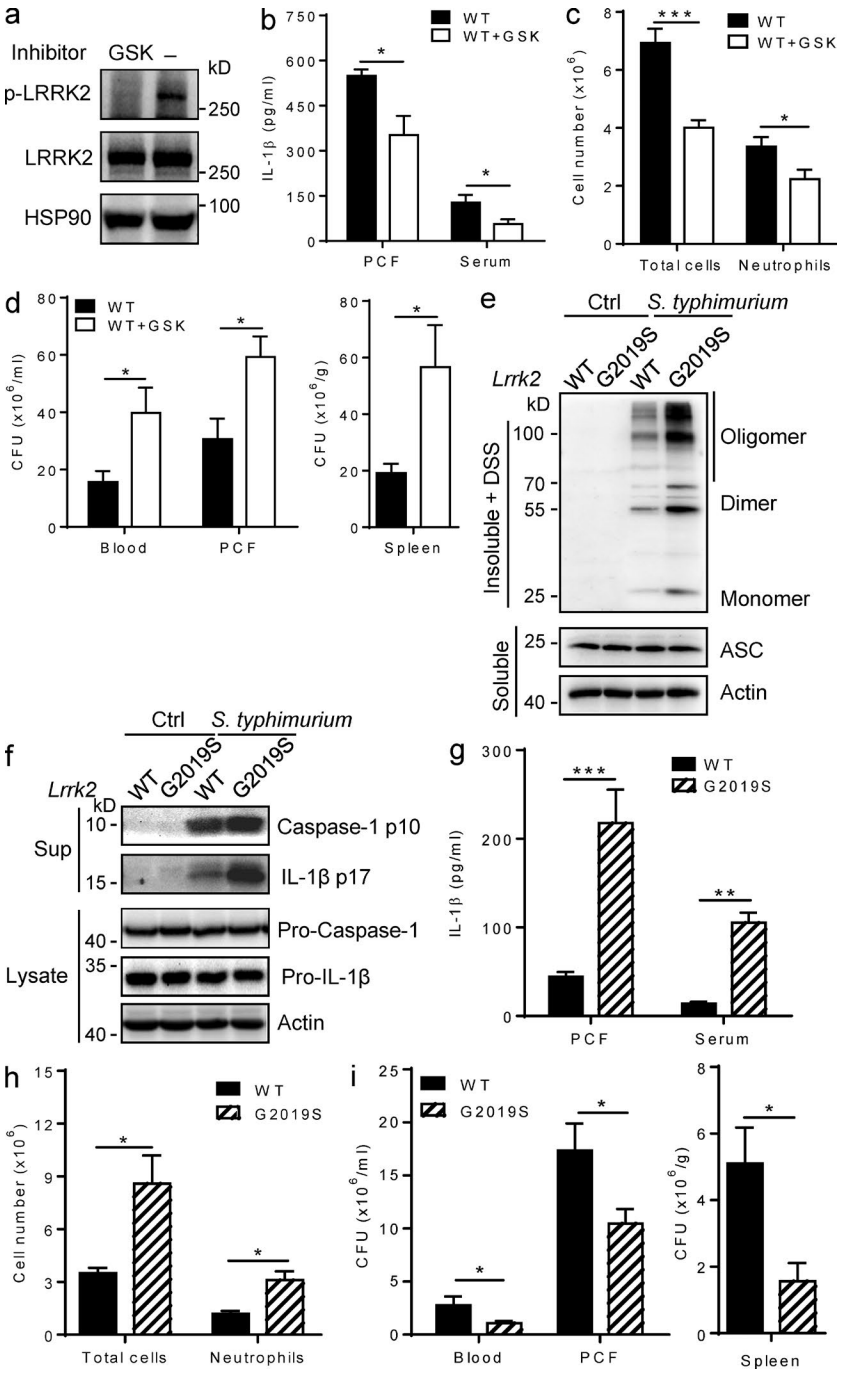

Figure 7. **LRRK2 kinase activity is required for host defense against *S.* Typhimurium infection.** (a) WT mice were intraperitoneally injected with LRRK2 inhibitor GSK2578215A (100 mg/kg) 1 h before *S.* Typhimurium infection. Peritoneal cells were collected for detecting LRRK2 phosphorylation 6 h after infection. (b) ELISA analysis of IL-1β levels in PCF and sera of WT and GSK2578215A-pretreated mice 6 h after *S.* Typhimurium infection. (c) Absolute number of total peritoneal cells and neutrophils ($CD11b^+$ $Ly6G^+$) from PCF of WT and GSK2578215A-pretreated mice 6 h after *S.* Typhimurium infection. (d) Bacterial burden in blood, PCF, and spleens of WT and GSK2578215A-pretreated mice 24 h after *S.* Typhimurium infection. (e) Peritoneal macrophages from littermate control (WT) and *LRRK2* G2019S transgenic mice were infected with *S.* Typhimurium at an MOI of 50 for 1 h. Cells were dissolved with Triton X-100–containing buffer followed by cross-linkage of insoluble fractions with DSS to capture ASC oligomers. Immunoblots of those insoluble fractions (Insoluble + DSS) and soluble fractions were detected with an antibody to ASC. (f) LPS-primed peritoneal macrophages from WT and *LRRK2* G2019S transgenic mice were infected with *S.* Typhimurium at an MOI of 100 for 2 h. Cell lysates and culture supernatants (Sup) were collected and blotted with the indicated antibodies. (g) ELISA analysis of IL-1β levels in PCF and sera from littermate control WT and *LRRK2* G2019S transgenic mice 6 h after *S.* Typhimurium infection. (h) Absolute number of total peritoneal cells and neutrophils ($CD11b^+$ $Ly6G^+$) from PCF of littermate control and *LRRK2* G2019S transgenic mice 6 h after *S.* Typhimurium infection. (i) Bacterial burden in blood, PCF, and spleens of littermate control and *LRRK2* G2019S transgenic mice 12 h after *S.* Typhimurium infection. Data are shown as means ± SEM; *, $P < 0.05$; **, $P < 0.01$; ***, $P < 0.001$; determined by Student's *t* test. All data are representative of three independent experiments, and $n = 5$ mice/group for each experiment.

ASC oligomerization assay

For the generation of Triton X-100–soluble and –insoluble fractions, differentially stimulated macrophages were lysed with 50 mM Tris-HCl, pH 7.6, containing 0.5% Triton X-100, EDTA-free protease inhibitor cocktail, and phosphatase inhibitor cocktail (Roche). The lysates were centrifuged at 6,000 *g* for 15 min at 4°C, and the pellets and supernatants were used as the Triton X-100–insoluble and –soluble fractions, respectively. For the detection of ASC oligomerization, the Triton X-100–insoluble pellets were washed twice with TBS buffer and then were resuspended in 300 µl TBS buffer. The resuspended pellets underwent cross-linkage for 30 min at room temperature with 2 mM DSS (Thermo Fisher Scientific) and then were centrifuged for 15 min at 6,000 *g*. The pellets were dissolved in SDS sample buffer and subjected to immunoblotting.

NLRC4 inflammasome reconstitution in HEK293T cells

HEK293T cells were plated in six-well microplates and incubated overnight. The cells were transfected with plasmids

expressing Flag-tagged human pro–IL-1β (500 ng/well), pro–caspase-1 (300 ng/well), and NLRC4 (500 ng/well) with or without plasmid-encoding Myc-tagged *LRRK2* (1,500 ng/well) or its mutants *LRRK2* G2019S and D2017A using Lipofectamine 2000. The total amount of DNA was adjusted through the use of empty vector. Cells were collected 24 h after transfection and lysed in NP-40 buffer (50 mM Tris, pH 7.6, 150 mM NaCl, 1% [vol/vol] NP-40, and complete protease inhibitors). IL-1β maturation was assessed by immunoblot analysis.

Immunoprecipitation and immunoblot

24 h after transient transfection as described in Fig. 4 (b and d–f), Fig. 5 (d and e), Fig. 6 d, and Fig. S2 a, HEK293T cells were lysed in cold NP-40 lysis buffer (50 mM Tris, pH 7.6, 150 mM NaCl, 1% [vol/vol] NP-40, and complete protease inhibitors). Cell lysates were incubated with anti-Flag or anti-Myc antibody at 4°C. The proteins bound by antibody were pulled down by protein A/G magnetic beads (Biotool) and subjected to immunoblot analysis. For the endogenous interaction assay, macrophages were lysed with NP-40 lysis buffer with complete protease inhibitor. The cell lysates were incubated with anti-LRRK2 antibody and protein A/G magnetic beads at 4°C. For immunoblot analysis, all protein samples were dissolved in SDS sample buffer and resolved by 7.5–15% SDS-PAGE. After electrophoresis, separated proteins were transferred onto polyvinylidenedifluoride membrane (EMD Millipore). The membrane was then blocked with 5% nonfat milk. After incubation with specific primary antibody, horseradish peroxidase–conjugated secondary antibody was applied. The positive immune reactive signal was detected by enhanced chemiluminescence (EMD Millipore).

Cross-linking

Peritoneal macrophages from *Lrrk2*$^{-/-}$ and WT mice were infected with *S.* Typhimurium at an MOI of 50 for 1–2 h. A cleavable imidoester cross-linker dimethyl 3,3′-dithiobispropionimidate-2HCl (DTBP) was added to cultures 30 min before cell lysis. Cell extracts were obtained by addition of NP-40 lysis buffer with complete protease inhibitor and then incubated with anti-ASC antibody and protein A/G magnetic beads at 4°C overnight.

In vitro kinase assays

In vitro kinase assays were performed either by mixing immunoprecipitated LRRK2 and NLRC4 in the kinase assay buffer for 60 min at 30°C or by incubating purified recombinant LRRK2 and NLRC4 protein in kinase buffer under the same conditions.

NLRC4 WT and S533A mutant purification: HEK293T cells transfected with plasmids expressing 3×Flag NLRC4 WT or S533A mutant were lysed in NP-40 lysis buffer. The cell lysates were incubated with anti-Flag antibody and protein A/G magnetic beads at 4°C. Beads was washed extensively with NP-40 lysis buffer with excessive salt concentration and eluted with 0.5 mg/ml 3×Flag peptide (Biotool) in PBS.

Purified recombinant LRRK2 (A15197) and PKCδ protein (P2293) were purchased from Invitrogen. Purified human LRKK2 (200 ng) or PKCδ protein (50 ng) were incubated with/without purified 3×Flag-NLRC4 WT or S533A mutant (50 ng) for kinase assays. The reaction was stopped by the addition of 2×SDS sample buffer and heating for 5 min at 95°C. Proteins were subjected to SDS-PAGE followed by immunoblotting for NLRC4 phosphorylation analysis.

In vitro pull-down assay

50 ng purified 3×Flag-NLRC4 protein was mixed with/without 200 ng recombinant LRRK2 protein and incubated with rabbit IgG or anti-LRRK2 antibody and protein A/G magnetic beads overnight at 4°C in cold NP-40 lysis buffer (50 mM Tris, pH 7.6, 150 mM NaCl, 1% [vol/vol] NP-40, and complete protease inhibitors). The beads were washed four times with NP-40 lysis buffer. The bound proteins were eluted from the beads by boiling in SDS-PAGE sample buffer. The eluted samples were subjected to immunoblot analysis. 10% of the mixture of LRRK2 and NLRC4 proteins was shown as input.

Immunofluorescence staining

Cells were treated as indicated. Cells were washed and fixed in 4% paraformaldehyde, permeabilized with 0.1% Triton X-100, and blocked with 1% BSA in PBS for 30 min. The cells were incubated with anti-ASC (Santa Cruz Biotechnology, Inc.) and then with Alexa Fluor 488–labeled antibody to rabbit IgG (Invitrogen). Nuclei were stained with DAPI. Confocal micrographs were imaged using an Eclipse confocal microscope (Nikon).

Mass spectrometry

HEK293T cells were transfected with plasmids expressing Flag-tagged human NLRC4 with or without plasmid-encoding human *LRRK2* using Lipofectamine 2000. Cell lysates were immunoprecipitated with anti-Flag and protein A/G magnetic beads. Proteins eluted with 3×Flag peptide were resolved by SDS-PAGE, and bands corresponding with NLRC4 were excised, reduced, alkylated, and digested with in situ trypsin. Tryptic peptides were analyzed with a QExactive hybrid quadrupole-Orbitrap mass spectrometer (Thermo Fisher Scientific). Tandem mass spectra were searched against a target protein database using the MASCOT search engine (Matrix Science Ltd).

RT-PCR and sequencing

LRRK2 G2019S transgenic mice and littermate control WT mice were sacrificed, and peritoneal macrophages and brains were subsequently separated and snap frozen on liquid nitrogen. RNA was isolated using TRIzol (Invitrogen) following the manufacturer's instructions. cDNA was synthesized with a PrimeScript RT Master Mix kit (Takara Bio Inc.). PCR was performed with Q5 High-Fidelity DNA Poly-

merase (New England Biolabs, Inc.). The primers for human-specific *LRRK2* (NM_198578.3) were 5′-AAGAGC TTGTGGTGCTTTGC-3′ and 5′-TGAGAGCTGTCC TCTGTCGG-3′; and mouse *GAPDH* (NM_001289726.1) primers were 5′-AGGTCGGTGTGAACGGATTTG-3′ and 5′-TGTAGACCATGTAGTTGAGGTCA-3′. The PCR products were analyzed by agarose gel electrophoresis and sequenced with the human *LRRK2* primers.

In vivo infection

For survival experiments, *Lrrk2*$^{-/-}$ and littermate control WT mice were infected intraperitoneally with 1×10^2 CFUs of *S.* Typhimurium, and mice survival was monitored daily. For the acute *S.* Typhimurium model, WT and *Lrrk2*$^{-/-}$ mice were infected with 1×10^7 CFUs *S.* Typhimurium for 6 h. Then, WT and *Lrrk2*$^{-/-}$ mice were sacrificed, and serum and PCF were collected for detection of IL-1β, IL-6, and TNF analysis by ELISA. Meanwhile, peritoneal cells were obtained, counted, and analyzed by flow cytometry. CD11b and Ly6G double-positive cells were identified as neutrophils. For bacterial burden analysis, 24 h after *S.* Typhimurium infection, WT and *Lrrk2*$^{-/-}$ mice were sacrificed, and then blood, PCF, and spleens were harvested, weighted, and homogenized. Systemic bacterial burdens were determined by plating dilutions on Luria-Bertani agar plates, then colonies were counted, and CFU/g of tissue was determined.

Statistical analysis

The p-values were determined by unpaired Student's *t* tests unless otherwise specified as in Figs. 2 e and 5 e, where a one-way ANOVA was used followed by Bonferroni's post hoc test. Survival rates were analyzed by the Kaplan-Meier method. P-values <0.05 were considered to be significant. All values are presented as means ± SEM unless otherwise specified.

Online supplemental material

Fig. S1 shows Coomassie blue staining of purified recombinant LRRK2 and NLRC4 proteins (NLRC4 WT and S533A mutant) and is related to Fig. 6. Fig. S2 indicates identification of phosphorylation at Ser533 of NLRC4 by mass spectrometry and is related to Fig. 6. Fig. S3 shows genotyping of *LRRK2* G2019S transgenic mice by RT-PCR and cDNA sequencing and is related to Fig. 7.

ACKNOWLEDGMENTS

We thank the Michael J. Fox Foundation for Parkinson's Research for the *LRRK2* gene knockout mice.

Z. Kang is supported by grants from the National Natural Science Foundation of China (DK30104150003 and DK30104150035), the Program for Professor of Special Appointment (Eastern Scholar) at Shanghai Institutions of Higher Learning, and the Shanghai Pujiang Program (2685721). W. Liu is supported by the China Postdoctoral Science Foundation (2014M560340).

The authors declare no competing financial interests.

Submitted: 3 January 2017
Revised: 20 May 2017
Accepted: 11 July 2017

REFERENCES

Amer, A., L. Franchi, T.D. Kanneganti, M. Body-Malapel, N. Ozören, G. Brady, S. Meshinchi, R. Jagirdar, A. Gewirtz, S. Akira, and G. Núñez. 2006. Regulation of *Legionella* phagosome maturation and infection through flagellin and host Ipaf. *J. Biol. Chem.* 281:35217–35223. http://dx.doi.org/10.1074/jbc.M604933200

Anderson, C.A., G. Boucher, C.W. Lees, A. Franke, M. D'Amato, K.D. Taylor, J.C. Lee, P. Goyette, M. Imielinski, A. Latiano, et al. 2011. Meta-analysis identifies 29 additional ulcerative colitis risk loci, increasing the number of confirmed associations to 47. *Nat. Genet.* 43:246–252. http://dx.doi.org/10.1038/ng.764

Arman, A., N. Isik, A. Coker, F. Candan, K.S. Becit, and E.O. List. 2010. Association between sporadic Parkinson disease and interleukin-1β -511 gene polymorphisms in the Turkish population. *Eur. Cytokine Netw.* 21:116–121.

Barrett, J.C., S. Hansoul, D.L. Nicolae, J.H. Cho, R.H. Duerr, J.D. Rioux, S.R. Brant, M.S. Silverberg, K.D. Taylor, M.M. Barmada, et al. Wellcome Trust Case Control Consortium. 2008. Genome-wide association defines more than 30 distinct susceptibility loci for Crohn's disease. *Nat. Genet.* 40:955–962. http://dx.doi.org/10.1038/ng.175

Broz, P., K. Newton, M. Lamkanfi, S. Mariathasan, V.M. Dixit, and D.M. Monack. 2010. Redundant roles for inflammasome receptors NLRP3 and NLRC4 in host defense against *Salmonella*. *J. Exp. Med.* 207:1745–1755. http://dx.doi.org/10.1084/jem.20100257

Case, C.L., S. Shin, and C.R. Roy. 2009. Asc and Ipaf Inflammasomes direct distinct pathways for caspase-1 activation in response to *Legionella pneumophila*. *Infect. Immun.* 77:1981–1991. http://dx.doi.org/10.1128/IAI.01382-08

Chen, K.W., C.J. Groß, F.V. Sotomayor, K.J. Stacey, J. Tschopp, M.J. Sweet, and K. Schroder. 2014. The neutrophil NLRC4 inflammasome selectively promotes IL-1β maturation without pyroptosis during acute *Salmonella* challenge. *Cell Reports.* 8:570–582. http://dx.doi.org/10.1016/j.celrep.2014.06.028

Chia, R., S. Haddock, A. Beilina, I.N. Rudenko, A. Mamais, A. Kaganovich, Y. Li, R. Kumaran, M.A. Nalls, and M.R. Cookson. 2014. Phosphorylation of LRRK2 by casein kinase 1α regulates trans-Golgi clustering via differential interaction with ARHGEF7. *Nat. Commun.* 5:5827. http://dx.doi.org/10.1038/ncomms6827

Cookson, M.R. 2010. The role of leucine-rich repeat kinase 2 (LRRK2) in Parkinson's disease. *Nat. Rev. Neurosci.* 11:791–797. http://dx.doi.org/10.1038/nrn2935

Cookson, M.R. 2015. LRRK2 pathways leading to neurodegeneration. *Curr. Neurol. Neurosci. Rep.* 15:42. http://dx.doi.org/10.1007/s11910-015-0564-y

Deng, X., N. Dzamko, A. Prescott, P. Davies, Q. Liu, Q. Yang, J.D. Lee, M.P. Patricelli, T.K. Nomanbhoy, D.R. Alessi, and N.S. Gray. 2011. Characterization of a selective inhibitor of the Parkinson's disease kinase LRRK2. *Nat. Chem. Biol.* 7:203–205. http://dx.doi.org/10.1038/nchembio.538

Dzamko, N., D.B. Rowe, and G.M. Halliday. 2016. Increased peripheral inflammation in asymptomatic leucine-rich repeat kinase 2 mutation carriers. *Mov. Disord.* 31:889–897.

Franchi, L., A. Amer, M. Body-Malapel, T.D. Kanneganti, N. Ozören, R. Jagirdar, N. Inohara, P. Vandenabeele, J. Bertin, A. Coyle, et al. 2006. Cytosolic flagellin requires Ipaf for activation of caspase-1 and interleukin 1β in salmonella-infected macrophages. *Nat. Immunol.* 7:576–582. http://dx.doi.org/10.1038/ni1346

Franke, A., D.P. McGovern, J.C. Barrett, K. Wang, G.L. Radford-Smith, T. Ahmad, C.W. Lees, T. Balschun, J. Lee, R. Roberts, et al. 2010. Genome-wide meta-analysis increases to 71 the number of confirmed Crohn's disease susceptibility loci. *Nat. Genet.* 42:1118–1125. http://dx.doi.org/10.1038/ng.717

Gardet, A., Y. Benita, C. Li, B.E. Sands, I. Ballester, C. Stevens, J.R. Korzenik, J.D. Rioux, M.J. Daly, R.J. Xavier, and D.K. Podolsky. 2010. LRRK2 is involved in the IFN-γ response and host response to pathogens. *J. Immunol.* 185:5577–5585. http://dx.doi.org/10.4049/jimmunol.1000548

Hara, H., K. Tsuchiya, I. Kawamura, R. Fang, E. Hernandez-Cuellar, Y. Shen, J. Mizuguchi, E. Schweighoffer, V. Tybulewicz, and M. Mitsuyama. 2013. Phosphorylation of the adaptor ASC acts as a molecular switch that controls the formation of speck-like aggregates and inflammasome activity. *Nat. Immunol.* 14:1247–1255. http://dx.doi.org/10.1038/ni.2749

Hu, Z., C. Yan, P. Liu, Z. Huang, R. Ma, C. Zhang, R. Wang, Y. Zhang, F. Martinon, D. Miao, et al. 2013. Crystal structure of NLRC4 reveals its autoinhibition mechanism. *Science.* 341:172–175. http://dx.doi.org/10.1126/science.1236381

Hu, Z., Q. Zhou, C. Zhang, S. Fan, W. Cheng, Y. Zhao, F. Shao, H.W. Wang, S.F. Sui, and J. Chai. 2015. Structural and biochemical basis for induced self-propagation of NLRC4. *Science.* 350:399–404. http://dx.doi.org/10.1126/science.aac5489

Inzelberg, R., O.S. Cohen, J. Aharon-Peretz, I. Schlesinger, R. Gershoni-Baruch, R. Djaldetti, Z. Nitsan, L. Ephraty, O. Tunkel, E. Kozlova, et al. 2012. The LRRK2 G2019S mutation is associated with Parkinson disease and concomitant non-skin cancers. *Neurology.* 78:781–786. http://dx.doi.org/10.1212/WNL.0b013e318249f673

Johnson, L.N., M.E. Noble, and D.J. Owen. 1996. Active and inactive protein kinases: Structural basis for regulation. *Cell.* 85:149–158. http://dx.doi.org/10.1016/S0092-8674(00)81092-2

Man, S.M., L.J. Hopkins, E. Nugent, S. Cox, I.M. Glück, P. Tourlomousis, J.A. Wright, P. Cicuta, T.P. Monie, and C.E. Bryant. 2014. Inflammasome activation causes dual recruitment of NLRC4 and NLRP3 to the same macromolecular complex. *Proc. Natl. Acad. Sci. USA.* 111:7403–7408. http://dx.doi.org/10.1073/pnas.1402911111

Masumoto, J., S. Taniguchi, K. Ayukawa, H. Sarvotham, T. Kishino, N. Niikawa, E. Hidaka, T. Katsuyama, T. Higuchi, and J. Sagara. 1999. ASC, a novel 22-kDa protein, aggregates during apoptosis of human promyelocytic leukemia HL-60 cells. *J. Biol. Chem.* 274:33835–33838. http://dx.doi.org/10.1074/jbc.274.48.33835

Matikainen-Ankney, B.A., N. Kezunovic, R.E. Mesias, Y. Tian, F.M. Williams, G.W. Huntley, and D.L. Benson. 2016. Altered development of synapse structure and function in striatum caused by Parkinson's disease-linked LRRK2-G2019S mutation. *J. Neurosci.* 36:7128–7141. http://dx.doi.org/10.1523/JNEUROSCI.3314-15.2016

Matusiak, M., N. Van Opdenbosch, L. Vande Walle, J.C. Sirard, T.D. Kanneganti, and M. Lamkanfi. 2015. Flagellin-induced NLRC4 phosphorylation primes the inflammasome for activation by NAIP5. *Proc. Natl. Acad. Sci. USA.* 112:1541–1546. http://dx.doi.org/10.1073/pnas.1417945112

Miao, E.A., I.A. Leaf, P.M. Treuting, D.P. Mao, M. Dors, A. Sarkar, S.E. Warren, M.D. Wewers, and A. Aderem. 2010a. Caspase-1-induced pyroptosis is an innate immune effector mechanism against intracellular bacteria. *Nat. Immunol.* 11:1136–1142. http://dx.doi.org/10.1038/ni.1960

Miao, E.A., D.P. Mao, N. Yudkovsky, R. Bonneau, C.G. Lorang, S.E. Warren, I.A. Leaf, and A. Aderem. 2010b. Innate immune detection of the type III secretion apparatus through the NLRC4 inflammasome. *Proc. Natl. Acad. Sci. USA.* 107:3076–3080. http://dx.doi.org/10.1073/pnas.0913087107

Nolen, B., S. Taylor, and G. Ghosh. 2004. Regulation of protein kinases: Controlling activity through activation segment conformation. *Mol. Cell.* 15:661–675. http://dx.doi.org/10.1016/j.molcel.2004.08.024

Paisán-Ruíz, C., S. Jain, E.W. Evans, W.P. Gilks, J. Simón, M. van der Brug, A. López de Munain, S. Aparicio, A.M. Gil, N. Khan, et al. 2004. Cloning of the gene containing mutations that cause PARK8-linked Parkinson's disease. *Neuron.* 44:595–600. http://dx.doi.org/10.1016/j.neuron.2004.10.023

Pott Godoy, M.C., R. Tarelli, C.C. Ferrari, M.I. Sarchi, and F.J. Pitossi. 2008. Central and systemic IL-1 exacerbates neurodegeneration and motor symptoms in a model of Parkinson's disease. *Brain.* 131:1880–1894. http://dx.doi.org/10.1093/brain/awn101

Qu, Y., S. Misaghi, A. Izrael-Tomasevic, K. Newton, L.L. Gilmour, M. Lamkanfi, S. Louie, N. Kayagaki, J. Liu, L. Kömüves, et al. 2012. Phosphorylation of NLRC4 is critical for inflammasome activation. *Nature.* 490:539–542. http://dx.doi.org/10.1038/nature11429

Qu, Y., S. Misaghi, K. Newton, A. Maltzman, A. Izrael-Tomasevic, D. Arnott, and V.M. Dixit. 2016. NLRP3 recruitment by NLRC4 during *Salmonella* infection. *J. Exp. Med.* 213:877–885. http://dx.doi.org/10.1084/jem.20132234

Reith, A.D., P. Bamborough, K. Jandu, D. Andreotti, L. Mensah, P. Dossang, H.G. Choi, X. Deng, J. Zhang, D.R. Alessi, and N.S. Gray. 2012. GSK2578215A; A potent and highly selective 2-arylmethyloxy-5-substitutent-*N*-arylbenzamide LRRK2 kinase inhibitor. *Bioorg. Med. Chem. Lett.* 22:5625–5629. http://dx.doi.org/10.1016/j.bmcl.2012.06.104

Rodrigues, M.C., P.R. Sanberg, L.E. Cruz, and S. Garbuzova-Davis. 2014. The innate and adaptive immunological aspects in neurodegenerative diseases. *J. Neuroimmunol.* 269:1–8. http://dx.doi.org/10.1016/j.jneuroim.2013.09.020

Rudenko, I.N., R. Chia, and M.R. Cookson. 2012. Is inhibition of kinase activity the only therapeutic strategy for LRRK2-associated Parkinson's disease? *BMC Med.* 10:20. http://dx.doi.org/10.1186/1741-7015-10-20

Saez-Atienzar, S., L. Bonet-Ponce, J.R. Blesa, F.J. Romero, M.P. Murphy, J. Jordan, and M.F. Galindo. 2014. The LRRK2 inhibitor GSK2578215A induces protective autophagy in SH-SY5Y cells: involvement of Drp-1-mediated mitochondrial fission and mitochondrial-derived ROS signaling. *Cell Death Dis.* 5:e1368. http://dx.doi.org/10.1038/cddis.2014.320

Saunders-Pullman, R., M.J. Barrett, K.M. Stanley, M.S. Luciano, V. Shanker, L. Severt, A. Hunt, D. Raymond, L.J. Ozelius, and S.B. Bressman. 2010. LRRK2 G2019S mutations are associated with an increased cancer risk in Parkinson disease. *Mov. Disord.* 25:2536–2541.

Schroder, K., and J. Tschopp. 2010. The inflammasomes. *Cell.* 140:821–832. http://dx.doi.org/10.1016/j.cell.2010.01.040

Shi, J., Y. Zhao, K. Wang, X. Shi, Y. Wang, H. Huang, Y. Zhuang, T. Cai, F. Wang, and F. Shao. 2015. Cleavage of GSDMD by inflammatory caspases determines pyroptotic cell death. *Nature.* 526:660–665. http://dx.doi.org/10.1038/nature15514

Sutterwala, F.S., L.A. Mijares, L. Li, Y. Ogura, B.I. Kazmierczak, and R.A. Flavell. 2007. Immune recognition of *Pseudomonas aeruginosa* mediated by the IPAF/NLRC4 inflammasome. *J. Exp. Med.* 204:3235–3245. http://dx.doi.org/10.1084/jem.20071239

Suzuki, T., L. Franchi, C. Toma, H. Ashida, M. Ogawa, Y. Yoshikawa, H. Mimuro, N. Inohara, C. Sasakawa, and G. Nuñez. 2007. Differential regulation of caspase-1 activation, pyroptosis, and autophagy via Ipaf and ASC in *Shigella*-infected macrophages. *PLoS Pathog.* 3:e111. http://dx.doi.org/10.1371/journal.ppat.0030111

Vance, R.E. 2015. The NAIP/NLRC4 inflammasomes. *Curr. Opin. Immunol.* 32:84–89. http://dx.doi.org/10.1016/j.coi.2015.01.010

Wahner, A.D., J.S. Sinsheimer, J.M. Bronstein, and B. Ritz. 2007. Inflammatory cytokine gene polymorphisms and increased risk of Parkinson disease. *Arch. Neurol.* 64:836–840. http://dx.doi.org/10.1001/archneur.64.6.836

Zhang, F.R., W. Huang, S.M. Chen, L.D. Sun, H. Liu, Y. Li, Y. Cui, X.X. Yan, H.T. Yang, R.D. Yang, et al. 2009. Genomewide association study of leprosy. *N. Engl. J. Med.* 361:2609–2618. http://dx.doi.org/10.1056/NEJMoa0903753

Zhang, L., S. Chen, J. Ruan, J. Wu, A.B. Tong, Q. Yin, Y. Li, L. David, A. Lu, W.L. Wang, et al. 2015a. Cryo-EM structure of the activated NAIP2-NLRC4 inflammasome reveals nucleated polymerization. *Science.* 350:404–409. http://dx.doi.org/10.1126/science.aac5789

Zhang, Q., Y. Pan, R. Yan, B. Zeng, H. Wang, X. Zhang, W. Li, H. Wei, and Z. Liu. 2015b. Commensal bacteria direct selective cargo sorting to promote symbiosis. *Nat. Immunol.* 16:918–926. http://dx.doi.org/10.1038/ni.3233

Zhao, Y., J. Yang, J. Shi, Y.N. Gong, Q. Lu, H. Xu, L. Liu, and F. Shao. 2011. The NLRC4 inflammasome receptors for bacterial flagellin and type III secretion apparatus. *Nature.* 477:596–600. http://dx.doi.org/10.1038/nature10510

Zimprich, A., S. Biskup, P. Leitner, P. Lichtner, M. Farrer, S. Lincoln, J. Kachergus, M. Hulihan, R.J. Uitti, D.B. Calne, et al. 2004. Mutations in *LRRK2* cause autosomal-dominant parkinsonism with pleomorphic pathology. *Neuron.* 44:601–607. http://dx.doi.org/10.1016/j.neuron.2004.11.005